In Pursuit of Advanced Materials from Single-Source Precursors Based on Metal Carbonyls†

Kenton H. Whitmire* and Desmond E. Schipper
Department of Chemistry, MS60
Rice University
6100 Main Street
Houston, Texas 77005

Abstract

In this perspective, the development of single-source precursors and their relative advantages over multiple source approaches for the synthesis of metal pnictide solid state materials is explored. Particular efforts in the selective production of iron phosphide materials for catalytic applications are discussed, especially directed towards the hydrogen evolution and oxygen evolution reactions of water splitting.

Introduction

Since the discovery of quantum dots (QDs) in the early 1980s, first by Alexei Ekimov in a glass matrix[1, 2] and shortly thereafter by Louis Brus in colloidal solution,[3] much attention has been focused on the synthesis of materials on the nanoscale owing to their unique quantum properties and consequent applications.[4, 5] The most highly studied of these have been the cadmium chalcogenide QDs, with later expansion into a large variety of other materials. To a large extent, however, many of the systems studied are simple in the sense that there is a limited composition and phase space for the crystalline target materials. The cadmium chalcogenides, for example, yield a 1:1 compound between the metal (M) and main group element (E), with the crystallites adopting either the cubic zinc blende or the hexagonal wurtzite lattice, which are only slightly different in energy. The situation among most transition metals in combination with main group elements, however, is much more complicated. This is illustrated in **Table 1** for the iron phosphides, where six distinct Fe:P stoichiometries have been identified and structurally characterized under ambient conditions. Crystal data for metal phosphides and related arsenides have been recently reviewed.[6] The challenge then, from the perspective of a synthetic inorganic chemist is, *"How do you produce selectively a single phase in a single crystal morphology in a such a complicated phase space?"* As far as we can tell, no systematic study of the catalytic properties of these compounds as a function of M:E stoichiometry has been conducted and remains a significant challenge.

†Electronic supplementary information (ESI) available: X-ray data for $\{Fe(CO)_2(^tBuPH_2)(\mu\text{-}^tBuPH)\}_2$ CCDC 1862751.

Table 1. The Binary Iron Phosphides					
Cmpd.	*Crystal System*	*Space Group*	*Cell Constants, Å*	*Properties*	*Ref.*
Fe_4P	Orthorhombic	*Pmmm* (#47)	*a* = 3.59(5) *b* = 4.01(5) *c* = 4.32(5)	unknown	[7]
Fe_3P	Tetragonal	$I\bar{4}$ (#82)	*a* = 9.1074(5) *c* = 4.4602(5)	Ferromagnetic T_C = 716K metallic[8]	[9]
Fe_2P	Hexagonal	$P\bar{6}2m$ (#189)	*a* = 5.8677(3) *c* = 3.4585(3)	Ferromagnetic T_C = 209K metallic[8]	[10, 11]
FeP	Orthorhombic	$Pna2_1$ (#33)	*a* = 5.193(1) *b* = 5.792(1) *c* = 3.099(1)	Antiferromagnetic T_N = 115K metallic[8]	[12]
FeP_2	Orthorhombic	*Pnnm* (#58)	*a* = 4.98732(5) *b* = 5.6590(5) *c* = 2.7235(3)	Diamagnetic Semiconductor E_{BG} = 0.37 eV[13]	[14]
FeP_4	Monoclinic	$P2_1/c$ (#14)	*a* = 4.619(1) *b* = 13.670(2) *c* = 7.002(1) β = 101.48(2)°	Semiconductor[8] (E_{BG},γ-FeP_4 = 1.0 eV)	[15]
	Monoclinic	*C2/c* (#15)	*a* = 5.043(7) *b* = 10.407(2) *c* = 11.069(2)		[16]
	Orthorhombic	$C222_1$ (# 20)	*a* = 5.005(1) *b* = 10.213(3) *c* = 5.530(1) β = 94.14(1)°		[17]

Why the Metal Pnictides?

While the principles discussed may be applied to the creation of E-M phases for a wide range of main group elements and transition metals, this article will focus on those of the transition metal phosphides (TMPs). It should be kept in mind that similar properties exist for many *p*-block element-transition metal combinations. Doping of compounds with other M or E elements has been effective in tuning a wide variety of properties. We first examine the utility of the metal phosphides that motivates their study. They have been known since the late 18th century when chemists were exploring fundamental reactions between recently discovered elements. After determining that metals would react with phosphorus sources in fixed ratios, very little was done with the TMPs until the mid 20th century when X-ray diffraction techniques permitted elucidation of the structures. It was realized that the TMPs were more than just combinatory mixtures of the elements but a discrete class of materials with each TMP having a unique structure, although these structures are similar between metals (See **Table 2**). Furthermore, these well-defined structures were

found to be the source of interesting properties, particularly magnetic and electronic properties. By the early 2000s, a number of researchers were turning their attention to the synthesis of nanoparticles based on M_xE_y phases for their potential electronic, magnetic and photonic applications.

There are significant synthetic challenges with these materials on the nanoscale. For each metal (M) and phosphide (P), there typically exist several phases M_xP_y possible, and even for a given M_xP_y there can be multiple crystallographic modifications as illustrated in **Table 2**. As a consequence, there is a significant challenge in producing a single phase cleanly.

The conventional synthesis of any given bulk M_xE_y is little different from the syntheses of the 18th century – heating the metal and pnictide in the ratios desired, often for long periods of time (multiple days) and at temperatures greater than 1000 K.[54,55] The method is complicated by the volatility of elemental E, so the reactions are most often done in sealed containers. To obtain these materials as ingots, often the air-sensitive powders are first prepared crudely by conventional methods, then arc-melted and quenched. The solid-state syntheses are constrained by the similarities in the thermodynamics of the formations of the possible phases, making it difficult to obtain a single-phase as a pure material easily, especially given the high temperatures of the reactions.

Over the past 20 years, additional methods of producing these phases have been explored such as phosphidization of metals, metal and metal oxide NPs, atomic layer deposition, reduction of metal phosphate compounds, reaction of Na_3P with metal halides, reaction of P_4 or red phosphorus with metal complexes, etc., but none of these methods offer the potential control over stoichiometry that is afforded by the metal carbonyls. For example, in the Co-P system where there are four known stable phases – Co_2P, CoP, CoP_2 and CoP_3 – only the first two have been observed in the reaction of cobalt metal with PPh_3 in spite of Co:PPh_3 ratios ranging from 4:1 to 1:4.[18] Similarly, only Fe_2P, FeP, Ni_2P and NiP_2 were obtained by the same method in spite of the existence of other possible phases.[18]

While not all metals form stable metal carbonyls, the elements in the first row transition series from Cr through Ni exhibit a large variety of phosphorus-containing metal carbonyl complexes, both mononuclear and cluster compounds, that could be employed as SSPs for the production of solid-state phosphide phases, and it is their utility as SSPs that has motivated our studies in this area for the past 15+ years.

Table 2. Comparison of the First Row Transition Metal Phosphide Phases.										
M:E Ratio	*3*	*4*	*5*	*6*	*7*	*8*	*9*	*10*	*11*	*12*
4:1						Fe_4P *Pmmm*			Cu_3P $P\bar{3}c1$	
3:1	Sc_3P *Pnma*	Ti_3P $P4_2/n$	V_3P $P4_2/n$	Cr_3P $I\bar{4}$	Mn_3P $I\bar{4}$	Fe_3P $I\bar{4}$	Co_3P $I\bar{4}$	Ni_3P $I\bar{4}$	Cu_3P $P\bar{3}m1$	
2.66:1								Ni_8P_3 *R3c*		
2.40:1								$Ni_{12}P_5$ *I4/m*		
2.33:1	Sc_7P_3 $P6_3mc$									
2:1		Ti_2P $P\bar{6}2m$	V_2P *Pnma*	Cr_2P *Imm2*	Mn_2P $P\bar{6}2m$	Fe_2P $P\bar{6}2m$	Co_2P $P\bar{6}2m$	Ni_2P $P\bar{6}2m$	Cu_3P $P6_3cm$	
						Fe_2P *Imm2*	Co_2P *Pnma*	Ni_2P $P32_1$		
1.75:1		Ti_7P_4 *C2/m*								
1.71:1				$Cr_{12}P_7$ $P\bar{6}$						
1.66:1		Ti_5P_3 $P6_3/mcm$	V_5P_3 $P6_3/mcm$							
		Ti_5P_3 *Pnma*								
1.5:1	Sc_3P_2 *Pnma*									Zn_3P_2 $Ia\bar{3}$
										Zn_3P_2 $P4_2/nmc$
										Zn_3P_2 $P4_232$
1.33:1		Ti_4P_3 $I\bar{4}3d$	V_4P_3 *Cmcm*							
1.25:1								Ni_5P_4 $P6_3mc$		

1:1	ScP *Fm$\bar{3}$m*	TiP *P6$_3$/mmc*	VP *P6$_3$/mmc*	CrP *Pnma*	MnP *Pnma*	FeP *Pnma*	CoP *Pnma*	NiP *Pbca*		
								NiP 1.29 GPa *Pbca*		
								NiP 5.79 GPa *Cmc2$_1$*		
								NiP 16.3 GPa *Pnma*		
								NiP 28.5 GPa *Cmc2$_1$*		
1:1.43										Zn_7P_{10} *Fdd2*
1:2		TiP_2 *Pnma*	VP_2 *C2/m*	CrP_2 *C2/m*		FeP_2 *Pnnm*	CoP_2 *P2$_1$/c*	NiP_2 *Pa$\bar{3}$*	CuP_2 *P2$_1$/c*	ZnP_2 *P4$_1$2$_1$2*
								NiP_2 *C2/c*		ZnP_2 monoclinic
1:3							CoP_3 *Im$\bar{3}$*	NiP_3 *Im$\bar{3}$*		
1:4			VP_4 *C2/c*	CrP_4 *C2/c*	MnP_4 *C2/c*	FeP_4 *C2/c*				ZnP_4 *P4$_1$2$_1$2*
					MnP_4 *P$\bar{1}$*	FeP_4 *C222$_1$*				
					MnP_4 *P$\bar{1}$*	FeP_4 *P2$_1$/c*				
1:3.5									Cu_2P_7 *C2/m*	
1:10									CuP_{10} *P$\bar{1}$*	

As with the free metals, the metal phosphides have interesting magnetic properties. The role of phosphorus in these materials has more to do with tuning the spacings and symmetry relations between the metals in the crystal structure than to contribute directly to the magnetic and electronic nature of these materials, although there is certainly a physicochemical contribution of the phosphorus to their mechano-elastic nature.[56] By tuning the distances between the metals, phosphorus alters both inter- and intra-layer coupling between metals within the crystal structure leading to Ferromagnetic (FM), Antiferromagnetic (AF), or paramagnetic (PM) states for the metal-rich phosphides. For the metal-poor phosphides, phosphorus acts to reduce the conductivity, opening up a bandgap.[35] In general, there are fewer M-M bonds if any in the phosphorus poor phases (M:P <1) and more M-M bonds with higher M:P ratios.[6] **Table 1** presents representative data for the iron phosphides as illustration of the effect of phosphorus on the magnetic and electronic properties. In spite of their availability, the physical properties of many of the transition metal phosphides have not been thoroughly examined, and further possibilities for tuning properties exist for compounds containing multiple metals and/or main group elements.

The Precursor Strategy

In the early 2000s, it occurred to us that the metal carbonyls could provide a solution to the synthetic challenge of producing a single, pure compound for a significant number of the target materials. Volatile metal carbonyl compounds have been known since the pioneering work of Ludwig Mond in the last decade of the 19th century when he reported the preparation of $Ni(CO)_4$, $Fe(CO)_5$ and '$Co(CO)_4$'.[19-21] Among his many industrial accomplishments was the application of these discoveries to the purification of nickel metal by decomposition of $Ni(CO)_4$ in what is known as the Mond process,[22] which showed that nickel carbonyl could also be readily converted back to the metallic elements and CO at elevated temperatures. Similarly, the heterometallic carbonyl clusters $H_2FeM_3(CO)_x$ (M = Ru, Os, x =13; M = Co, x = 12) were later shown to decompose on partially hydroxylated magnesia to yield bimetallic metal particles.[23]

In the years since Mond, the development of organometallic chemistry in general, and metal carbonyl cluster chemistry in particular, provided a good starting point for imagining the precursors that could be produced to target these complex phases. Another pioneer in this area was Walter Hieber, who explored the synthesis of many main group element-transition metal carbonyl combinations in the 1950s and 1960s and laid the groundwork for much of the metal carbonyl cluster chemistry that followed shortly thereafter, largely facilitated by the development of user-friendly single crystal X-ray diffractometers and structure solution & refinement software.[24, 25] A further stimulus to this research was the development of cluster bonding theories by Wade[26] and Mingos[27] and the 1981 Nobel Prize winning isolobal analogy developed by R. Hoffmann.[28, 29] Those theories provide the framework for systematic development of both homonuclear metal and main group element cluster chemistry as well as the hybrid E-M clusters that still serves well today. The structure and function relationships between clusters and solid-state metals was noted by Muetterties as early as 1975.[30]

The diversity of compositions in **Table 1** is mirrored by many other transition metal-main group element combinations. There is a fairly obvious divide in going from metal-rich to main group element-rich compositions in the type of precursors that would be most appropriate. Mononuclear complexes of the type $(CO)_nM(ER_x)_y$ where the complexes are generically simple-substituted compounds can readily be envisioned to serve as precursors to the E-rich phases. Specifically $(OC)_xML$ and $(OC)_XML_2$ (L = phosphine-based ligand) are obvious choices for preparation of 1:1 and 1:2 M:P phases (**I** – **VII**). Direct substitutions of metal carbonyls to achieve higher degrees of substitution are rare but alternate methods exist, for example, to prepare H_2FeL_4 that could be a suitable precursor to the FeP_4 phase.[31]

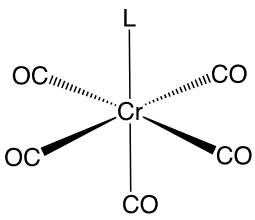

I

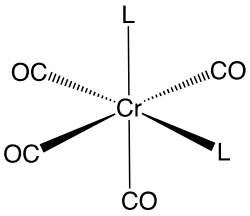

II

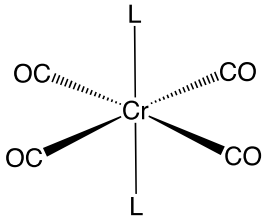

III

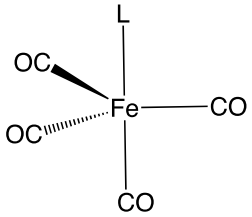

IV

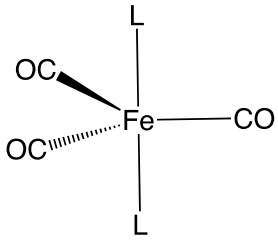

V

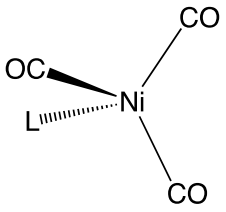

VI

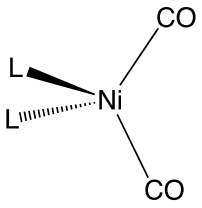

VII

The nature of the phosphine ligand, however, is crucial to the formation of suitable materials, as will be discussed shortly, and significant synthetic challenges exist forming the corresponding complexes that have not been previously reported with primary and secondary phosphines. Use of main group element-rich cluster compounds could offer some advantages as SSPs in providing a more stable compositional framework (*vide infra*) but these are a much less-studied class of compounds.

In contrast, if one wants to prepare metal-rich phases, metal carbonyl clusters are the clear choice. These may be suitable for M:E ratios as low as 1:1. Examples that are suitable for 1:1 to 4:1 phases are shown as **VIII** - **XIV**. There is tremendous opportunity here for construction of a large number of different stoichoimetries in both E and M compositions. The metals do not have to be the same, and the R groups can be varied extensively or replaced by a lone pair of electrons. The only stipulation is that the electron counts and orbital structures of the fragments used correspond to the requirements of the isolobal analogy, with a few notable exceptions. Thus $HFe(CO)_3$ is equivalent to a

$Co(CO)_3$ fragment, and S, Se or Te is equivalent to a P-R group. An exception is the relationship between $H_2Fe_3(CO)_9(\mu_3\text{-}PR)$ and $Co_3(CO)_9(\mu_3\text{-}PR)$, where the latter is isostructural to the former but not isoelectronic. The cobalt compound is a rare example of a stable odd-electron carbonyl cluster. Nevertheless, both homonuclear and heteronuclear compounds can be formed by appropriate fragment replacement using now standard organometallic strategies. A caveat, however, is that even though these target compounds are reasonable and have ample literature precedent, synthetic methods to particular combinations may not work and not all combinations of M, E and R have been reported in the literature. Synthetic routes may not be straightforward regardless of the wealth of literature on cluster compounds that has been published in the last 50 years.

1:1 compounds

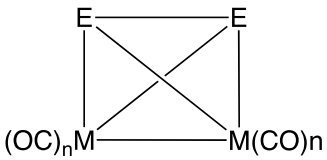

VIII

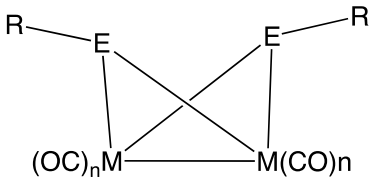

IX

2:1 compounds

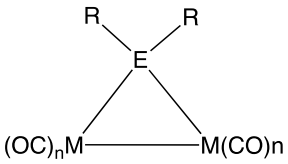

X

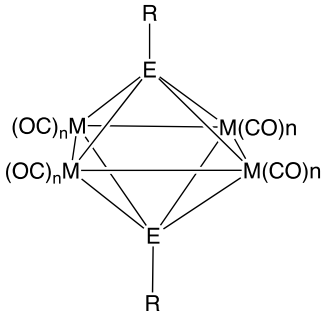

XI

3:1 Compounds

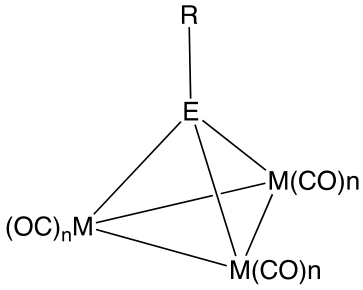

XII

4:1 compounds

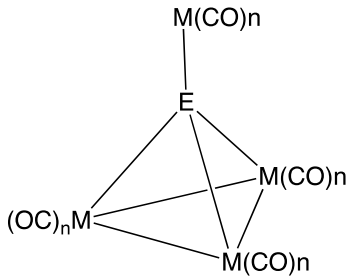

XIII

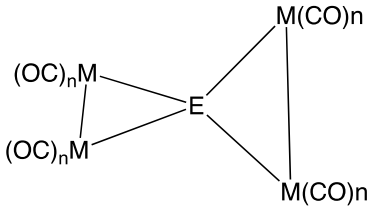

XIV

One criticism of the use of these compounds as precursors is the quantities that may be available, which is based largely on the early pot-boiling days of the field where heating of the suitable main group element reagents with metal carbonyls often led to complex mixtures of products that were difficult to separate. There are now a number of high yield routes available to produce compounds in useful quantities. For nanoparticle syntheses, the use of either neutral or anionic cluster compounds can be employed, but for thin film growth of materials by metal organic vapor deposition (MOCVD), neutral molecules that are often volatile are the molecules of choice.

Principles for preparing the target SSPs

As will be seen in the following discussion of NP and thin film syntheses, selecting suitable target SSPs involves creating molecules with some specific attributes:

1. Volatility is important for the use as conventional MOCVD sources, so initial targets have focused initially on neutral compounds. This is not a strict requirement for NP synthesis, but counter ions can impact NP growth. Not having them simplifies NP synthesis studies.
2. Organic functionalities on E should be restricted to clean leaving groups (e.g., H, ^{t}Bu).
3. Phosphines with electron-donating groups such as ^{t}Bu bind more strongly to the metals than PH_3, owing to higher donor abilities of the former.
4. Primary phosphines appear to decompose more cleanly than tertiary analogues.
5. Ligand sets are generally restricted to H and CO so that ligand loss from the metals is facile.

There are now a number of general routes to creating pnictide-containing metal carbonyl compounds. Simple substitution reactions of parent carbonyls (**Equation 1**) can readily be employed, although many of the known reactions have utilized tertiary phosphine compounds (PR_3). The R group of choice is ^{t}Bu as illustrated by $H_2Fe_3(CO)_9(\mu_3\text{-}P^{t}Bu)$, where clean elimination of isobutylene was accompanied by nicely formed Fe_2P

nanorods. In contrast, the use of Ph as an organic substituent, which is much more common among known compounds, has proven problematic for nanoparticle syntheses. Often decompositions with Ph substituents do not lead to quality nanoparticles. This was observed for decomposition of $FeMn(CO)_8(\mu\text{-}PPh_2)$ and $FeMn(CO)_8(\mu\text{-}PHPh)$, which gave no useful products. Clean production of FeMnP was observed, however, using $FeMn(CO)_8(\mu\text{-}PH_2)$. In the case of $H_2Fe_3(CO)_9(\mu_3\text{-}PPh)$ decomposition is accompanied by the elimination of benzene, and the NPs that resulted were poorer in quality with more irregular structures. Crystal splitting was also observed when hydrocarbons are introduced into this synthesis, and benzene could directly promote crystal splitting. Additionally, Ph must leave in a radical process and radicals could also promote crystal splitting.[32]

$$M(CO)_x \xrightarrow[-CO]{+PR_3} M(CO)_{x-1}(PR_3) \xrightarrow[-CO]{+PR_3} M(CO)_{x-2}(PR_3)_2 \quad (1)$$

$$Fe_3(CO)_{12} \xrightarrow[-3CO]{+PH_2R} H_2Fe_3(CO)_9(\mu_3\text{-}PR) \quad (2)$$

$$FeX_2 \xrightarrow{+4PR_3} Fe(PR_3)_4X_2 \xrightarrow{+LiAlH_4} H_2Fe(PR_3)_4 \quad (3)$$

There are definite advantages for primary phosphines PH_2R in promoting clean decomposition, as well as being lighter in mass to contribute to higher volatility. There are, however, very few metal carbonyl complexes reported for the primary phosphines, partially owing to the reactivity of the P-H bonds which can lead to higher nuclearity cluster formation as exemplified in **Equation 2**. For $Fe(CO)_5$ substitution generally stops at two phosphine ligands introduced, although other routes exist for higher order substitutions as in **Equation 3**, but surprisingly these more highly substituted compounds are unknown for primary phosphines. Primary phosphines have the added advantage of possessing reactive P-H bonds that can be used for further syntheses of higher nuclearity compounds, which could also be a reason why metal carbonyls substituted with multiple primary phosphines are rare.

A particularly important, related methodology is the deprotonation of primary phosphines to give anionic $[(M(CO)_x(PHR)]^-$ or $[(M(CO)_x(PR_2)]^-$ species that can be treated with metal carbonyl halides in nucleophilic displacement processes. This approach was employed to produce the $FeMn(CO)_8(\mu\text{-}PR_2)$ compounds exemplified in **Equation 4** and **Figure 1**. The development of syntheses to produce compounds with only hydrogen bound to phosphorus was important in being able to product FeMnP nanoparticles cleanly, and this compound proved to be an effective SSP for thin film production as well.

$$Fe(CO)_4(PHRR') \xrightarrow{base} [Fe(CO)_4(PRR')]^- \xrightarrow{Mn(CO)_5Br} FeMn(CO)_8(\mu\text{-}PRR')$$

$$R = R' = Ph;\ R = H,\ R' = Ph;\ R = R' = H \quad (4)$$

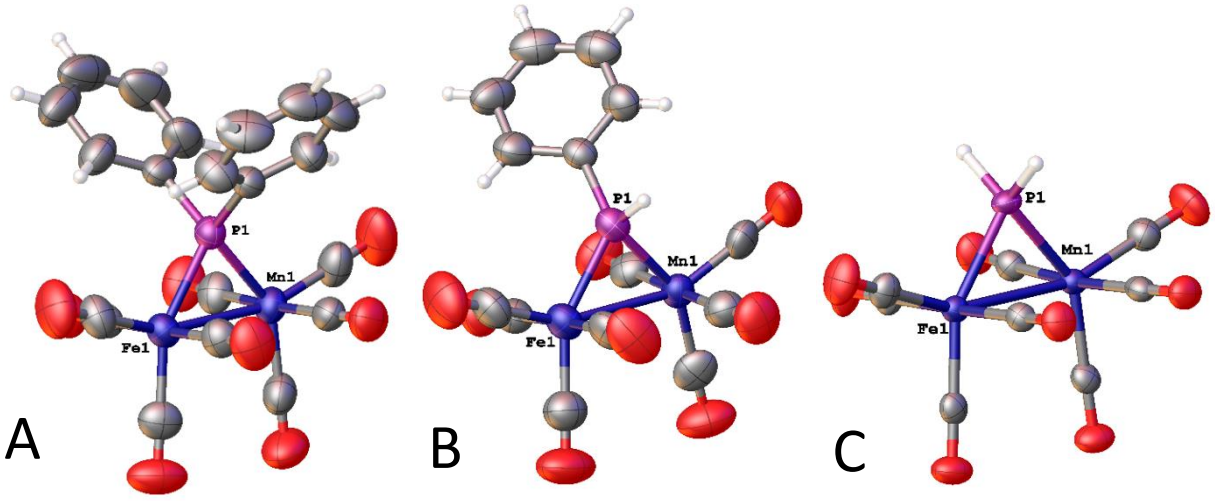

F**igure 1.** Crystal Structures of (A) $FeMn(CO)_8(\mu\text{-}PPh_2)$, (B) $FeMn(CO)_8(\mu\text{-}PPhH)$, and (C) $FeMn(CO)_8(\mu\text{-}PH_2)$.[33]

Our attempts to produce the simple disubstituted compound $Fe(CO)_3(PH_2{}^tBu)_2$ for use as a precursor to FeP_2 led unexpectedly to the dinuclear compound show in **Figure 2**, which could also be a viable precursor to this phosphorus-rich iron compound.

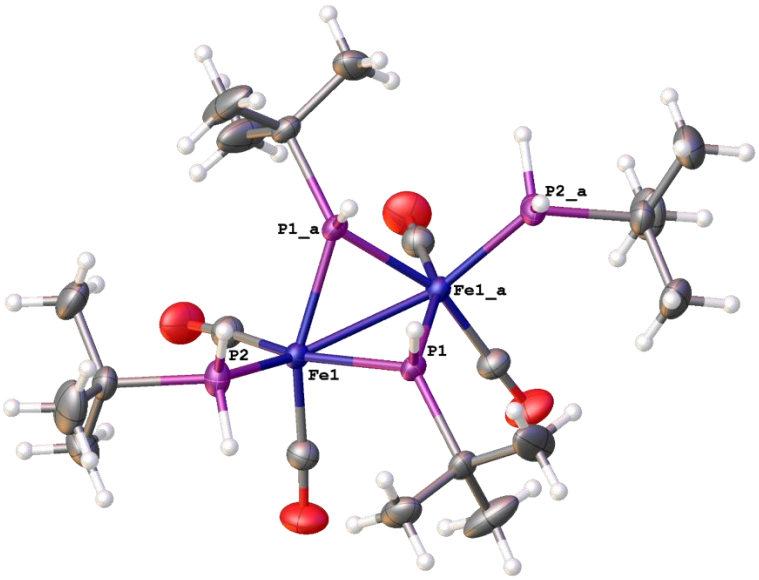

Figure 2. The crystal structure of $[Fe(CO)_2(^tBuPH_2)(\mu\text{-}^tBuPH)]_2$. Ellipsoids given at 50% probability. Details on the synthesis and crystal structure determination of

$[Fe(CO)_2(^tBuPH_2)(\mu\text{-}^tBuPH)]_2$ are given in the CIF file on deposit with the Cambridge Crystallographic Data Centre.

In addition to substitution processes, reaction of metal carbonyl anions with main group element halides and organohalides often results in nucleophilic displacement of the halides and the formation of E-M bonds. This has become a standard first method of introducing main group functionalities into metal carbonyl systems. It has long been known that reaction of metal carbonyl dianions with organophosphorus dihalides could result in "inidene" types of compounds containing a P-P multiple bond. In pursuing alternative ways to these compounds, mixtures of $[Fe(CO)_4]^{2-}$ and $[HFe(CO)_4]^-$ were treated with $PCl_2{}^tBu$, a dinuclear P-P single bonded compound $[^tBuP(H)Fe(CO)_4]_2$ compound was obtained (**Figure 3**).[34] This molecule is interesting from a structural standpoint owing to the various isomers available owing to the chirality at each phosphorus atom. It also can serve as an SSP to FeP as will be seen below.

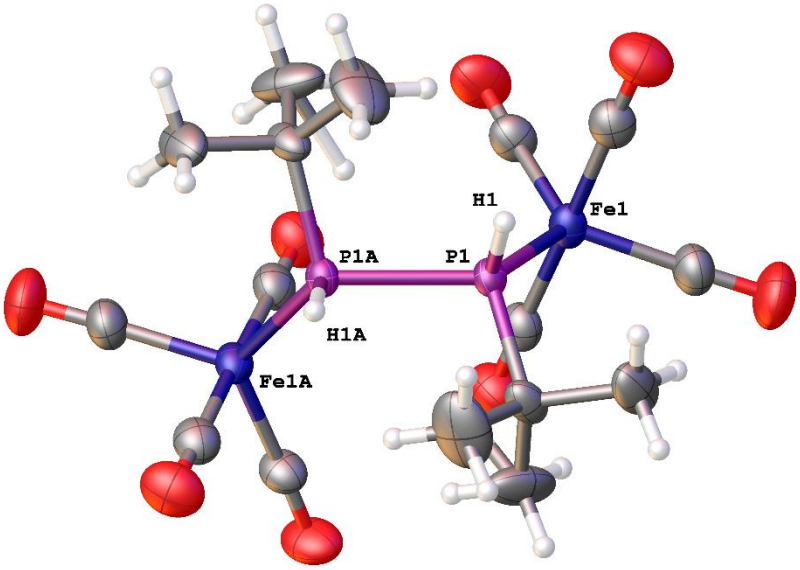

Figure 3. The structure of $[^tBuP(H)Fe(CO)_4]_2$.[34]

Advanced deposition techniques using, for example, electrospray for ionic precursors is possible but has not yet been evaluated. It is anticipated that this method may result in impurity issues with other atoms such as C and N, but proper experimental conditions, including an appropriate choice of counterion, may reduce that concern and open up the processes to a wider range of potential SSPs.

SSP Conversion to Materials

Lessons from Nanoparticle Syntheses:

Many of the early syntheses of metal phosphide nanoparticles (NPs) followed the protocols for the cadmium chalcogenide quantum dots. A soluble metal complex can be co-decomposed with a suitable E-containing organic compound, such as tri-n-

octylphosphine (TOP) as illustrated in **Table 3**. Brock and coworkers performed an extensive study on controlling the production of FeP versus Fe_2P by varying the time and reaction temperature.[35] In addition to producing NPs in solution by this method, M_2P (M = Mn, Co, Ni) have been prepared directly on carbon nanotubes coated with polyphosphazene.[36] Surprisingly, there is a very narrow range of stoichiometries accessible by these methods.

Table 3. Metal Phosphide Nanoparticle Syntheses from Metal Complexes

Phase Produced	*Metal Source*	*Surfactant/Phopshine Source*	*Morphology*	*Ref.*
MnP	$Mn_2(CO)_{10}$	TOPO/TOP	rods	[37]
MnP	$Mn_2(CO)_{10}$	$P(SiMe_3)_3$	spherical	[38]
CoMnP	$Mn_2(CO)_{10}$ + $Co_2(CO)_8$	TOP octadecene and oleylamine	spherical	[39]
FeP	$Fe(CO)_5$	tri-n-octylphosphine oxide/TOP	rods/wires	[40]
FeP	$Fe(acac)_3/FeCl_3$	$P(SiMe_3)_3$	spherical	[41, 42]
FeP	$Fe(CO)_5$	octadecene + oleyl amine/TOP	spherical	[35]
Fe_2P	$Fe(CO)_5$	octadecene + oleyl amine/TOP	rods	[35]
$(Fe,Ni)_2P$	$Fe(CO)_5$, $Ni(acac)_2$	TOP	rods	[43]
Co_2P	$Co(acac)_2$	hexadecylamine/TOP	rods	[37]
CoP	Co_2P NPs	TOP	hollow spheres	[44]
Co_2P	Co NPs	TOP	spheres	[44]
Co_2P	Co NPs	TOPO	hyperbranched NPs	[45]
Ni_2P	$Ni(acac)_2$	TOPO/TOP	rods, spherical	[37, 46, 47]
$Ni_{12}P_5$	$Ni(acac)_2$	TOPO/TOP	spherical	[47]

TOPO = tri-n-octylphosphine oxide

Silica-based aerogels with embedded metal phosphide NPs were prepared for Fe_2P, RuP, Co_2P, Rh_2P Ni_2P, Pd_5P_2 and PtP_2 from complexes of the metals with

$PR_2CH_2CH_2Si(OEt)_3$ (R = Ph, Et).[48] These complexes were first hydrolyzed to give gels that were subsequently treated at 600 - 900°C. Unfortunately, the metal to phosphorus ratios in the molecular precursors did not match the stoichiometry of the final NPs.

In order to overcome the limitations in M:E stoichiometry presented by these early metal phosphide NP syntheses, we turned our attention to the production of an as-yet-unknown iron phosphide stoichiometry in NP form. We reasoned that $H_2Fe_3(CO)_9(\mu_3\text{-}PR)$ should make an ideal precursor for the formation of Fe_3P NPs.[32] Fe_3P is a room temperature ferromagnetic material (T_C = 716 K). In comparison, Fe_2P is also ferromagnetic but has a T_C of 209 K, while FeP is antiferromagnetic with T_N = 115 K. When these syntheses were carried out in the conventional surfactant system of oleic acid and tri-n-octylamine with R = Ph, ^{t}Bu, the resulting particles in all cases were pure Fe_2P as nanorods and various aggregates of nanorods (**Figure 4A**). The R = ^{t}Bu precursor gave the best quality nanocrystals. Initially, we believed that cluster degradation and interconversion processes resulted in loss of the 3:1 stoichiometry before decomposition to NPs occurred, but later we discovered that these compounds react with oleic acid with the elimination of metal. Thus, bulk Fe_3P when treated with the same surfactant system at elevated temperatures produced Fe_2P, and Fe_2P in turn gave FeP, which reacted further to produce iron phosphate and oxide compounds. The obvious solution to this problem was to eliminate the oleic acid from but the resulting particles proved to be very small (<5 nm) and thus difficult to confirm unambiguously as the Fe_3P phase, although ICP analyses confirmed the expected 3:1 Fe:P stoichiometry and the particles appear to be strongly magnetic at room temperature.

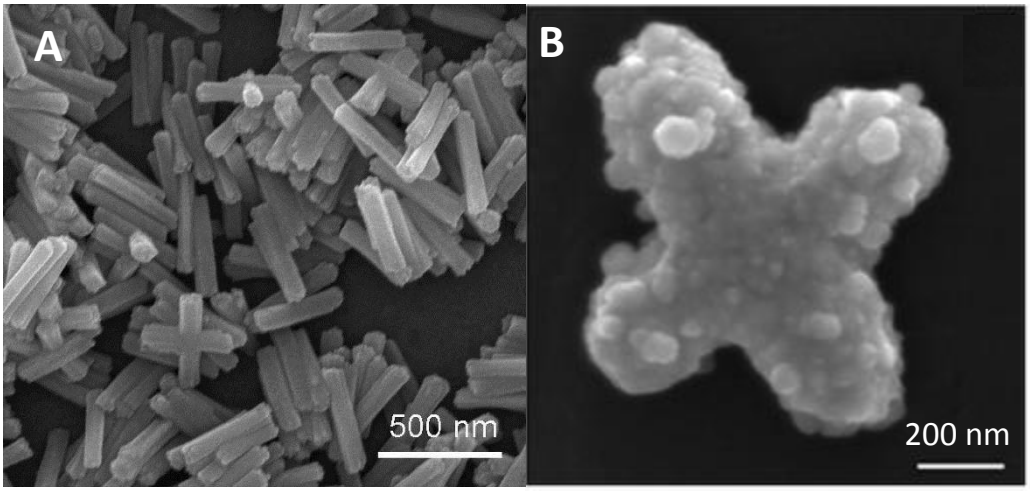

Figure 4. SEM images of A) Fe_2P nanorods and nanocrosses from the decomposition of $H_2Fe_3(CO)_9(\mu_3\text{-}P^tBu)$. Reproduced with permission from A. T. Kelly, I. Rusakova, T. Ould-Ely, C. Hofmann, A. Luettge and K. H. Whitmire, *Nano Lett.*, 2007, **7**, 2920-2925. and B) Gold-coated Fe_2P nanocross. Reproduced from A. T. Kelly, C. S. Filgueira, D. E. Schipper, N. J. Halas and K. H. Whitmire, *RSC Adv.*, 2017, **7**, 25848-25854.

The resulting Fe_2P nanorods and nanobundles can be coated with a gold shell to produce photonic materials (**Figure 4B**).[49] In order to get the Au seed particles to adhere to the

NPs, their surface coating that was presumably oleate had to be replaced with the bifunctional γ-aminobutyric acid (GABA). The pendant amine group provides the anchor for gold seed NPs that were grown into a full shell by reduction of chloroauric acid upon treatment with either formaldehyde or CO. The plasmon resonance red-shifted with increased Au-shell thickness.

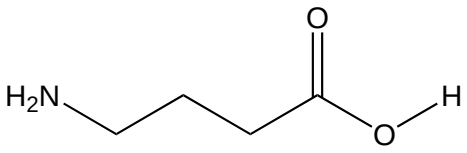

GABA

Examination of the more complex ternary phase FeMnP was also pursued.[50] The initial choice of precursor was $FeMn(CO)_8(\mu\text{-}PPh_2)$ already known in the literature[51, 52] but attempts to produce FeMnP NPs resulted only in the isolation of iron oxide NPs, presumably resulting from the strength of the P-C bonds. Replacement of one Ph group with hydrogen giving $FeMn(CO)_8(\mu\text{-}PHPh)$ was attempted with the hopes of providing a more favorable decomposition route - benzene elimination - but no NPs of any kind were isolated from that system under comparable conditions. Efforts were then directed to the synthesis of $FeMn(CO)_8(\mu\text{-}PH_2)$ whose decomposition in surfactants led to the desired FeMnP, although the stoichiometries were always manganese poor, consistently in the range of $Fe_{1.3}Mn_{0.7}P$.[50] Based on the experience from the Fe_3P system, it was rationalized that the presence of oleic acid was again not innocent, and the preferential loss of Mn compared to Fe was explained by the higher oxophilicity of the former metal. Further study showed more Mn loss with increased oleic acid content, and at the opposite extreme the exact stoichiometry of Fe:Mn:P could be obtained with no acid present. However, the resulting nanoparticles were tiny spheres (<~10 nm) as opposed to well-formed nanorods. Bulk decomposition of $FeMn(CO)_8(\mu\text{-}PH_2)$, however, led to stoichiometric FeMnP in the metastable hexagonal phase. These results point to the added complexity of working with heterometallic systems where the redox properties of the individual metals can have a profound effect on the outcome of the decomposition. Such details are masked in homometallic systems where the relative reactivities of the various metals will not be evidenced in the makeup of the products as noticeably.

Since those initial studies, others have examined SSPs as a means of producing metal phosphides. Scheer examined the decomposition of $Fe(CO)_4PH_3$, which rearranges to form the dinuclear bridged species $[(CO)_3Fe(\mu\text{-}PH_2)]_2$ for the production of FeP nanoparticles in surfactants.[53] The related complex $[(CO)_4Cr(\mu\text{-}PH_2)]_2$ was employed for synthesis of CrP.[54] Interestingly, decomposition of $[(CO)_4Mo(\mu\text{-}PMe_2)_2W(CO)_4]$ (M = Mo; M′ =W) led to metal oxide nanoparticles rather than a metal phosphide,[55] which is similar to our observations for the decomposition of $FeMn(CO)_8(\mu\text{-}PPh_2)$.

Bulk decomposition under H_2/N_2 (5/95%) of $[Co_4(CO)_{10}(\mu\text{-dppa})]$ (dppa = $HN(PPh_2)_2$) or $[Co_4(CO)_{10}(\mu_4\text{-}PPh)_2]$ led to Co_2P while use of the more highly substituted $[Co_4(CO)_8(\mu\text{-dppa})_2]$ resulted in CoP.[56] The compound $[Co_4(CO)_{10}(\mu\text{-dppa})]$ could be adsorbed onto

silica and converted into supported Co_2P NPs on the order of 5.5 – 6.5 nm but the sample was contaminated with some cobalt metal.[57] These NPs were shown to be superparamagnetic.

Summary

- *Single-source molecular carbonyl compounds with phosphorus-based ligands can be decomposed in surfactants to produce metal phosphide nanoparticles.*
- *In a number of cases, the final stoichiometry in the NP does not match the stoichiometry of the SSP.*
- *The surfactant system can be non-innocent as oleic acid was demonstrated to be responsible for the selective reduction in metal content of some NPs.*
- *In heterometallic systems, the different redox properties of the metals may lead to preferentially leaching of one metal. More oxophilic metals are more prone to leaching by carboxylic acids, ostensibly because of their higher affinity for oxo-based ligands.*
- *While oleic acid is a problematic surfactant medium because of leaching issues, it does promote crystalline NP growth.*

Thin Film Syntheses

In order to circumvent the problems of loss of SSP stoichiometry in the final products, we turned our attention to the production of thin films using the same SSPs as employed for NP synthesis. Previous efforts to produce thin films of transition metal-main group alloys including borides, nitrides, phosphides, silicides, and stannides from metal carbonyls are summarized in **Table 4**. The elemental ratios were roughly preserved for the borides, sulfides, and stannides. The boride Fe_3B produced from $HFe_3(CO)_9BH_4$ by sublimation onto a target substrate followed by pyrolysis was found to be amorphous under the conditions tested and oxygen-rich, which the authors attributed to being due to a low-quality vacuum. The silicide films prepared from $Co(CO)_4SiH_3$, $Fe(CO)_3(SiH_3)_2$, and $Mn(CO)_5SiH_3$ reported were found to be silicon poor,[58] likely due to the loss of SiH_4 or transiently stable siloxanes formed from the reaction of SiH_x with carbon monoxide. CoSn was achieved by use of $Co(CO)_4SnMe_3$, albeit with significant amounts of carbon present. The nitride γ-Fe_4N was obtained along with α-Fe in a 1:1 ratio by sublimation of $HFe_4(CO)_{12}N$ onto a glass substrate followed by pyrolysis. Here, the nitrogen content was below that expected for a 4:1 Fe to N ratio, and the authors could not account for how the nitrogen had left even after analysis of the waste gases, but they could not rule out loss of N_2. Iron sulfide films with an approximate 1:1 Fe:S stoichiometry were achieved using $Fe_2(CO)_6(\mu\text{-}S_2)$; however, the authors obtained a mixture of $Fe_{1-x}S_x$ and Fe_7S_8, likely due to the similar stoichiometries of the two phases.

Table 4. Thin Films of Borides, Nitrides, Silicides, and Stannides produced from Metal Carbonyl SSPs

	Thin Film Material	Precursor	Method	Substrate	Ref.
Borides	amorphous Fe_3B	$HFe_3(CO)_9BH_4$	Sublimation/Pyrolysis	Glass or Al	59
Nitrides	α-Fe & γ-Fe_4N	$HFe_4(CO)_{12}N$	Sublimation/Pyrolysis	Glass	60
Phosphides	$Cr_{12}P_7$, CrP	$Cr(CO)_5PH_3$	LPCVD	Pyrex	61
	Fe_2P	$Fe(CO)_4PH_3$	LPCVD	SiO_2 and FTO	62
	FeP	$Fe(CO)_4P^tBuH_2$ or $\{Fe(CO)_4(\mu\text{-}P^tBuH)\}_2$	LPCVD	SiO_2 and FTO	62
	Fe_3P	$H_2Fe_3(CO)_9(\mu\text{-}P^tBu)$	LPCVD	SiO_2	63
	FeMnP	$FeMn(CO)_8(\mu\text{-}PH_2)$	LPCVD	SiO_2, Al_2O_3, FTO, TiO_2/FTO, NF, Graphene	64 65 66
Silicides	CoSi, amorphous Co	$Co(CO)_4SiH_3$	Flow pyrolysis	Silica	58
	β-$FeSi_2$, amorphous Fe	$Fe(CO)_3(SiH_3)_2$	Flow pyrolysis	Silica	58
	MnSi/Mn_5Si_3	$Mn(CO)_5SiH_3$	Flow pyrolysis	Silica	58
Sulfides	$Fe_{1-x}S$, Fe_7S_8	$Fe_2(CO)_6(\mu\text{-}S_2)$	LPCVD	Si(100)	67
Stannides	CoSn	$Co(CO)_4SnMe_3$	LPCVD	Si(100)	68
	CoSn/Co_3Sn_2	$Co(CO)_4SnPh_3$	LPCVD	Si(100)	68

LDCVD = Low-pressure chemical vapor deposition; NF = Nickel Foam;

The earliest demonstration of a metal carbonyl-based precursor to a metal phosphide was the production of chromium-phosphorus films from $Cr(CO)_5PH_3$ by Watson and Connor (**Table 5**).[61] The films obtained were phosphorus-deficient and consisted of a mixture of $Cr_{12}P_7$ and CrP, perhaps due to the loss of PH_3.

The first phase-pure metal phosphide thin film to be grown was Fe_3P using $H_2Fe_3(CO)_9(\mu_3\text{-}P^tBu)$ as the SSP.[63] In many cases, the crystallinity of the films is improved by annealing the films. Details varied from material to material and substrate to substrate and the reader is referred to the original articles for specific conditions. Here, the intimate

bonding between P and Fe is likely to have assisted in the conservation of the Fe:P ratio from precursor to final material. Doped films were prepared using isostructural metal carbonyl clusters with other M or E atoms whose similar structural and electronic parameters were expected to confer on them similar volatilities.[69] Blends of $H_2Fe_3(CO)_9(\mu_3\text{-}P^tBu)$ with either $Co_3(CO)_9(\mu_3\text{-}P^tBu)$ or $H_2Fe_3(CO)_9(\mu_3\text{-}Te)$ (**Figure 5**) were prepared by dissolving the respective compounds in tetrahydrofuran followed by evaporation to yield intimate mixtures of the respective molecules. These blends could then be used to achieve doped Fe_3P, namely $(Fe_{1-x}Co_x)_3P$ ($0.09<x<0.22$) and $Fe_3(P_{1-x}Te_x)$ ($0.04<x<0.42$) with elemental compositions tunable by altering the molecular ratios in the blends. This strategy allows for the synthesis of phase-pure materials with complex stoichiometries, which will likely prove useful for advanced applications.

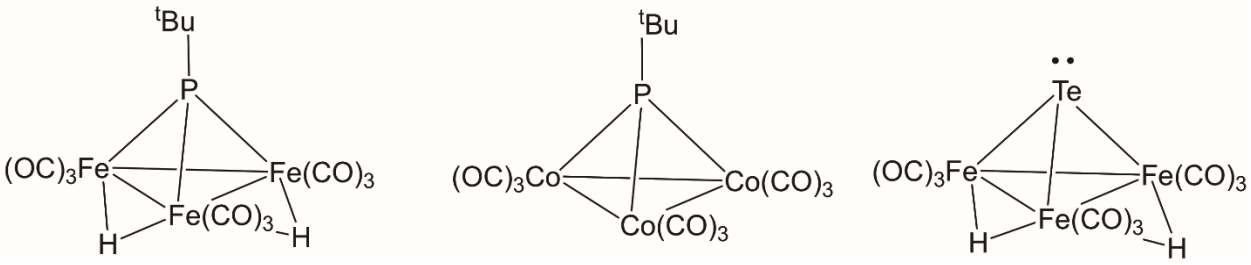

Figure 5: Isostructural metal carbonyl clusters used to prepare SSP-blends.[101]

In order to probe the thin film production of the other Fe-P phases, $Fe(CO)_4PH_3$, which had been shown by Scheer to serve as an SSP to FeP, was evaluated as a precursor to FeP. Low decomposition temperatures (350 ^oC) yielded Fe_2P as the sole phase with PH_3 detected in the off-gases.[62] The same precursor was shown to give a mixture of Fe_2P and FeP at higher temperatures (450 ^oC), similar to the decomposition behavior of $Cr(CO)_5PH_3$. This suggests that Cr_2P might be accessible at lower temperatures from $Cr(CO)_5PH_3$. Similarly, films obtained from $Fe(CO)_4P^tBuH_2$ at lower temperatures (350 ^oC) were found to be pure Fe_2P, but at higher temperatures pure FeP was formed. At the higher temperatures, the stronger binding of $^tBuPH_2$ as compared to that of PH_3 may play a role in eliminating phosphorus. Using $\{Fe(CO)_4\}(\mu\text{-}PH^tBu)\}_2$ as the SSP instead of $Fe(CO)_4P^tBuH_2$ resulted in FeP production even at 350 ^oC, likely because of the more intimate bonding the phosphorus ligands in the bridging configuration.

FeMnP was grown on a variety of substrates using $FeMn(CO)_8(\mu\text{-}PH_2)$ representing the first deposition of a heterobimetallic metal phosphide from a single-source precursor.[64-66] Initial difficulties were encountered in preparing the films on glass or quartz without the oxidation of Mn. In the limiting scenario, the films were shown to be completely uniform films of FeP and MnO. Originally, this was thought to arise from problems in the vacuum line being used; however, repeated trials could reduce but never eliminate the oxidation problem. Ultimately it was discovered that the SiO_2 substrate was the issue, and use of metal oxides, such as alumina, F-doped tin oxide (FTO) or titania, or metals such as nickel foam did not have these oxidation issues. This is consistent with the observation in the NP synthesis of FeMnP that Mn was preferentially leached out to produce NPs that were

richer in iron than Mn. As with the NP syntheses described above, the thin films of FeMnP also adopted the metastable hexagonal phase.

Summary

- Similar to the NP syntheses, thin films of TMPs can be prepared from volatile SSPs.
- Thin films doped with either M or E can be prepared by co-deposition of the majority SSP and an isostructural compound in which either E or M (or possibly both) has been introduced.
- Similar to NP synthesis where the surfactant system could be non-innocent, substrates with certain combinations of metals can also be reactive with the growing film.

Catalytic Properties of the TMPs as NPs and Thin Films

The TMPs are well-known as hydroprocessing and hydrogen evolution catalysts and as pre-catalysts for oxygen evolution catalysis. The hydroprocessing abilities, specifically hydrodenitrogenation (HDN) and hydrodesulfurization (HDS) have been known since the late 1990s.[64,65] Their use in this application lies in the resistance of the TMPs to decomposition or transformation in the presence of sulfur and nitrogen compounds, their hydrogenation capacity which helps remove sulfur and their ability to displace nitrogen from nitrogen-containing compounds through nucleophilic substitution.[66] HDN and HDS catalysis is vitally important to the chemical industry to remove sulfur and nitrogen from petrochemical feedstocks as nitrogen and sulfur compounds lead to corrosion of transport pipelines, contamination of feedstocks, poisoning of other catalysts, and environmentally-unfriendly off-gases if the sulfur is not removed before utilization in combustion engines. Despite these capabilities other catalyst systems appear to be preferred for commercial HDN and HD processes.

More recently, however, the discovery of the ability of the TMPs to catalyze the conversion of water into hydrogen and oxygen ("water-splitting") created an explosion of research into the utility of the metal phosphides for this purpose and the activity for homometallic and heterometallic compounds are summarized in **Tables 4** and **5**. Water electrolysis holds promise as a means of storing intermittent energy from solar and wind power generation in the form of hydrogen fuel, which of course converts to electricity and water when utilized in a fuel cell.

The TMPs are now well-known hydrogen evolution reaction (HER) electrocatalysts. Experimental evidence for the TMPs' HER activity was provided in early 2013 by Xu and coworkers with the report of high activity of FeP for the HER,[70] although this was preceded by a theoretical calculation for Ni_2P in 2006, itself inspired by high HER activity observed in molecular nickel-phosphine complexes.[71] Since then, many of the binary metal phosphides and even ternary metal phosphides have been evaluated as HER catalysts, with the respective performances rivaling platinum, the benchmark HER catalyst.[39, 72-86]

The TMPs also catalyze the oxygen-evolution reaction, although technically not directly. Rather, the TMPs convert to metal oxy-hydroxides at their surfaces,[87] which is not entirely surprising considering the basic conditions typically employed for water electrolysis and the oxidizing potentials used at the electrolysis anode. But, these oxyhydroxides are actually the best catalysts for oxygen-evolution. A distinct advantage for anodes built from metal phosphides is that the TMPs are conductive such that, even after the surface converts to metal oxyhydroxide, a conductive core is retained allowing current to flow to the active surface sites during electrolysis operation.

Table 5. Water-splitting catalytic activity of the homometallic transition metal phosphides: Blue = OER Catalyst; **Red** = HER Catalyst; **Purple** = Bifunctional Catalyst

Group:	**4**	**6**	**8**	**9**	**10**	**11**	**12**
First Row	TiP[88]		FeP_2[89] FeP[62, 70, 73, 74, 90] Fe_2P[62, 91, 92] Fe_3P[62]	Co_2P[93, 94] CoP[95] CoP_2[96]	Ni_5P_4[97] Ni_2P[98] Ni_3P[99]	Cu_3P[100]	β-ZnP_2[101]
Second Row		MoP_2[102] MoP[103] Mo_3P[104]	Ru_2P[105]	Rh_2P[106]			
Third Row		WP[107] WP_2[108]					

Table 6. Known Ternary Metal Phosphides Tested for HER, OER, or Both.

OER Catalyst	**HER Catalyst**	**Bifunctional Catalyst**
$CrTiP$[88]	$(Co_{1-x}V_x)P$[109]	$FeMnP$[66]
$MnTiP$[88]	$(Co,Mn)P$[110]	$CoFeP$[111]
$FeTiP$[88]	$(Ni_{1-x}Mn_x)P_2$[112]	$(Fe_{1-x}Ni_x)_2P$[113-115]
$CoTiP$[88]	$(Co,Fe)P$[116]	$(Co, Ni)P$[117]
$NiTiP$[88]	$NiZnP$[118]	$CoNiP$[82]
$CoMnP$[39]	$(Mo_{1-x}W_x)P_2$[119]	$(Co_{1-x}Mo_x)P$[120]
$(Fe_{1-x}Ni_x)_{12}P_5$[121]		$NiCuP$[122]
$NiWP$[123]		$NiMoP_2$[124]
$(Ni_{1-x}Ru_x)_2P$[125]		

SSP-Derived Thin Film Catalysis

Study of the metal pnictides has until recently been limited to magnetic studies on bulk materials leaving much of the phase-dependent surface physicochemical properties unexplored. The SSP-CVD method offers the ability to change that by allowing access to phase-pure materials with very low or negligible C and O, providing routes to surface chemistry comparisons between specific phases. The ability to grow the metal-phosphides on substrates of choice also facilitates easy property evaluation, especially important for electrochemical testing. For example, we determined the relative hydrogen evolution activities of FeP, Fe_2P, and Fe_3P grown on fluorine-doped tin oxide (FTO), a conductive substrate, using SSPs for each phase (**Figure 6**).[62] This platform of comparison led us to conclude iron-rich phosphide phases outperformed iron-poor phase for the hydrogen evolution reaction, of importance as alternative catalysts to Pt are currently in demand to satisfy growing global clean energy needs. The ability to form these phases in pure form should also allow more detailed and accurate examination of other phase-dependent properties.

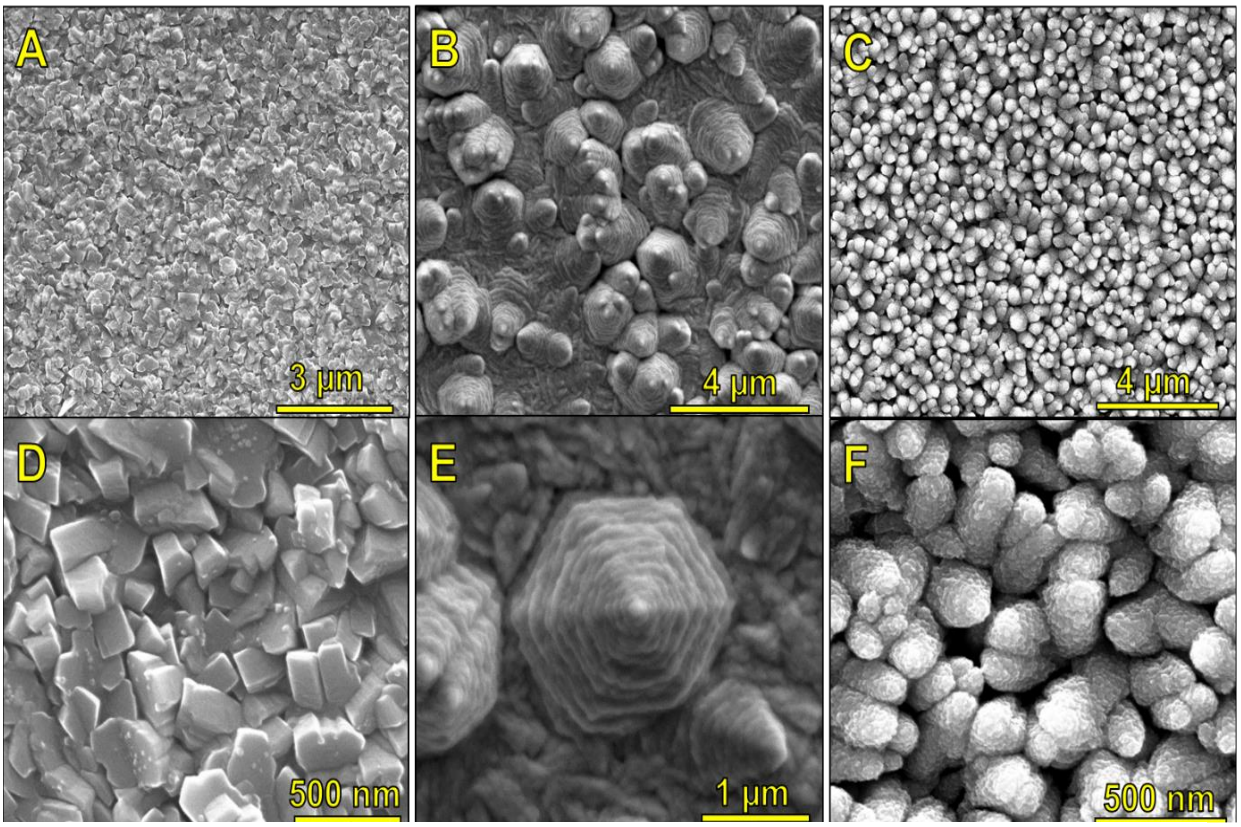

Figure 6. SEM images of FeP (A) and (D), Fe_2P (B) and (E), and Fe_3P (C) and (F) on FTO. Reproduced with permission from D. E. Schipper, Z. Zhao, H. Thirumalai, A. P. Leitner, S. L. Donaldson, A. Kumar, F. Qin, Z. Wang, L. C. Grabow, J. Bao and K. H. Whitmire, *Chem. Mater.*, 2018, 30, 3588-3598**.**

A further use of the SSP-CVD method is that of coatings for advanced applications, and the SSPs can readily be decomposed onto patterned substrates (**Figure 7**). The best

demonstration of this use was the conformal coating of FeMnP on a TiO_2 nanorod array for water-splitting applications for which it was found that FeMnP formed an excellent ohmic contact with the TiO_2 nanorods, facilitating fast charge migration of photogenerated holes.[65] When used to generate oxygen for the OER of water-splitting, this photoanode operated at the theoretical maximum for rutile TiO_2. These results reflect the performance achievable when a high-performance catalyst is grown directly on a semiconductor. The SSP-CVD method should prove very useful for mating high-performance TMPs with other semiconducting substrates.

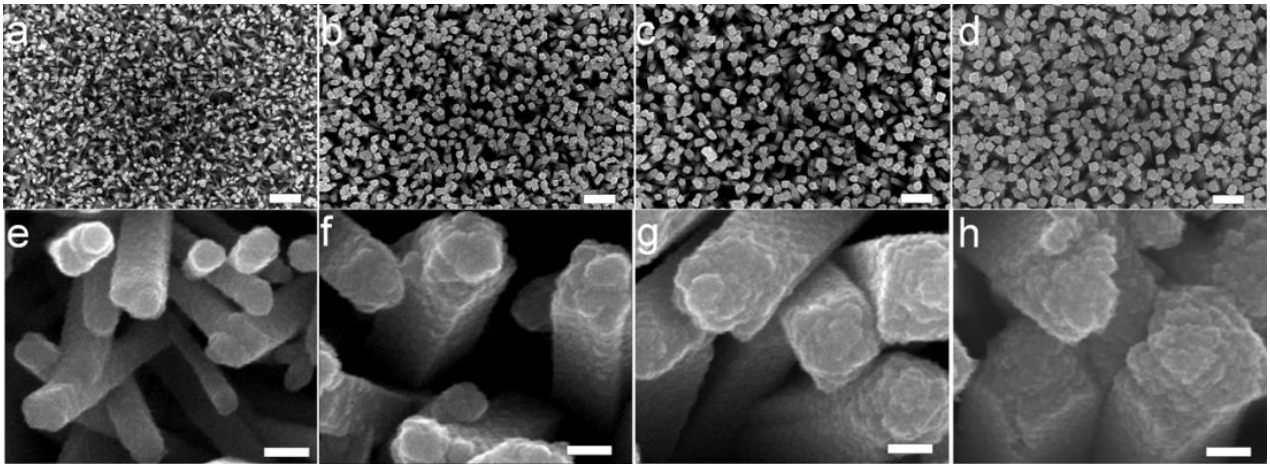

Figure 7. TiO_2/FeMnP core/shell nanorod arrays with different FeMnP loading amounts by changing the amount of precursor. (a) and (e) 2 mg precursor, (b) and (f) 5 mg precursor, (c) and (g) 10 mg precursor, (d) and (h) 20 mg precursor. The scale bar in (a)-(d) is 1 μm, and 100 nm in (e)-(h).[65] Reproduced with permission from D. E. Schipper, Z. Zhao, A. P. Leitner, L. Xie, F. Qin, M. K. Alam, S. Chen, D. Wang, Z. Ren, Z. Wang, J. Bao and K. H. Whitmire, *ACS Nano*, 2017, 11, 4051-4059.

The SSP-CVD method was also used to grow FeMnP on nickel foam (FeMnP/NF) and graphene-wrapped nickel foam (FeMnP/GNF) for bifunctional water splitting (**Figure 8**).[66] Both FeMnP/NF and FeMnP/GNF electrodes could be used "bifunctionally" where a single type of electrode, e.g. FeMnP/NF could be used for both hydrogen evolution and oxygen evolution. An electrolytic cell composed of two FeMnP/GNF electrodes split water at 1.51 V for 10 $mA \cdot cm^{-2}$ of current density placing it among the best bifunctional electrodes devised. The authors were able to determine the OER and HER characteristics of FeMnP because of its phase-purity and the high quality, conductive nature of the substrate. Moreover, the substrate was 3d-dimensional and porous, and complete coverage was achieved. One can imagine FeMnP or other metal pnictides being grown on the internal surface of porous materials for use in catalyst beds for industrial processes.

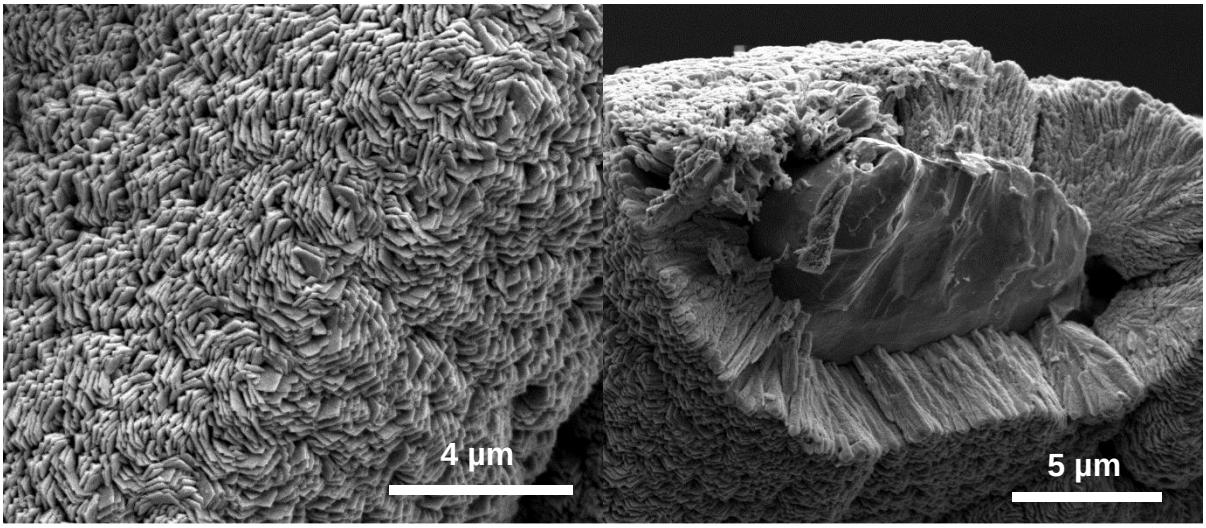

Figure 8. SEM Images of FeMnP grown on GNF. Typical Surface Morphology (Left), Cross-Section (Right).

Conclusions

Phase-pure metal phosphides can readily be grown as thin films on many substrates – including structured three-dimensional ones - with maximal surface coverage and good contact. They have proven particularly effective for electrocatalysis by allowing definitive comparisons between various metal phosphide phases for first time. The TMP films growth method is particularly appealing because the materials for the metal-rich phases are conductive, enhancing the catalytic performance of the materials. Furthermore, stoichiometry control has been achieved to a degree that has not been achieved by existing NP synthesis methods or other techniques such as atomic layer deposition, and the phosphidization of metal nanoparticles or metal surfaces. Patterned substrates as well as semiconductors can readily be coated using this technology, and this capability has opened the door to using the TMPS as photoelectrocatalysts for water splitting. The method can readily be extended to systematical evaluation of a range of metal pnictides for a host of catalytic applications where metal carbonyl pnictide compounds with the appropriate stoichiometry can be prepared based on standard organometallic methods and the isolobal analogy. Thus, the metal carbonyl cluster system affords a convenient starting point for producing phase-pure materials for a large range of other transition metal compositions. Additionally, the decomposition may proceed with kinetic control giving rise to metastable phases.

Conflicts of interest

There are no conflicts of interest to declare.

Acknowledgements

The authors thank Rice University, the National Science Foundation (CHE-1411495, KHW), and the Robert A. Welch Foundation (C-0976, KHW) for funding. This material is based upon work supported by the National Science Foundation Graduate Research Fellowship (DES) under Grant No. 1450681.

References

1. A. I. Ekimov and A. A. Onushchenko, *Pis'ma Zh. Eksp. Teor. Fiz.*, 1981, **34**, 363-366.
2. A. I. Ekimov and A. A. Onushchenko, *Fiz. Tekh. Poluprovodn. (Leningrad)*, 1982, **16**, 1215-1219.
3. R. Rossetti and L. Brus, *J. Phys. Chem.*, 1982, **86**, 4470-4472.
4. A. P. Alivisatos, *ACS Nano*, 2008, **2**, 1514-1516.
5. J. Li and J.-J. Zhu, *Analyst*, 2013, **138**, 2506-2515.
6. J.-H. Chen and K. H. Whitmire, *Coord. Chem. Rev.*, 2018, **355**, 271-327.
7. E. Hornbogen, *Trans. ASM*, 1961, **53**, 569-589.
8. J. Wu, X. Chong, R. Zhou, Y. Jiang and J. Feng, *RSC Advances*, 2015, **5**, 81943-81956.
9. P. H. Spriggs, *Philos. Mag.*, 1970, **21**, 897-901.
10. H. Fujii, S. Komura, T. Takeda, T. Okamoto, Y. Ito and J. Akimitsu, *J. Phys. Soc. Jpn.*, 1979, **46**, 1616-1621.
11. B. Carlsson, M. Gölin and S. Rundqvist, *J. Sol. State Chem.*, 1973, **8**, 57-67.
12. K. Selte and A. Kjekshus, *Acta Chem. Scand.*, 1972, **26**, 1276-1277.
13. G. Boda, B. Stenström, V. Sagredo, O. Beckman, B. Carlsson and S. Rundqvist, *Physica Scripta*, 1971, **4**, 132.
14. H. Holseth and A. Kjekshus, *Acta Chem. Scand.*, 1968, **22**, 3284-3292.
15. W. Jeitschko and D. J. Braun, *Acta Crystallogr. B*, 1978, **34**, 3196-3201.
16. S. Fiechter, H. Tributsch, M. Evain and R. Brec, *Mater. Res. Bull.*, 1987, **22**, 543-549.
17. M. Sugitani, N. Kinomura, M. Koizumi and S. Kume, *J. Solid State Chem.*, 1978, **26**, 195-201.
18. J. Wang, Q. Yang, Z. Zhang and S. Sun, *Chemistry – A European Journal*, 2010, **16**, 7916-7924.
19. L. Mond, H. Hirtz and M. D. Cowap, *Chem. Zentralbl.*, 1908, **79 Book 2**, 1491.
20. L. Mond and C. Langer, *J. Chem. Soc., Trans.*, 1891, **59**, 1090-1093.
21. L. Mond, C. Langer and F. Quincke, *J. Chem. Soc., Trans.*, 1890, **57**, 749-753.
22. P. Morris, *Endeavour*, 1989, **13**, 34-40.
23. A. Choplin, L. Huang, A. Theolier, P. Gallezot, J. M. Basset, U. Siriwardane, S. G. Shore and R. Mathieu, *J. Am. Chem. Soc.*, 1986, **108**, 4224-4225.
24. D. F. Shriver and K. H. Whitmire, in *Comprehensive Organometallic Chemistry*, ed. G. Wilkinson, Pergamon Press, Oxford, UK, 1982, vol. 31, ch. 1, pp. 243-329.
25. H. Whitmire Kenton, in *Comprehensive Organometallic Chemistry II*, eds. Abel, E.W., F. G. A. Stone and G. Wilkinson, Elsevier Science, Ltd., Oxford, UK, 1995, vol. 7, pp. 1-100.

26. K. Wade, *J. Chem. Soc., Chem. Comm.*, 1971, DOI: 10.1039/C29710000792, 792-793.
27. D. M. P. Mingos, *Nature Phys. Sci.*, 1972, **236**, 99.
28. R. Hoffmann, *Angew. Chem. Int. Ed. Eng.*, 1982, **21**, 711-724.
29. M. Elian, M. M. L. Chen, D. M. P. Mingos and R. Hoffmann, *Inorg. Chem.*, 1976, **15**, 1148-1155.
30. E. L. Muetterties, *Bulletin des Sociétés Chimiques Belges*, 1975, **84**, 959-986.
31. D. H. Gerlach, W. G. Peet and E. L. Muetterties, *J. Am. Chem. Soc.*, 1972, **94**, 4545-4549.
32. A. T. Kelly, I. Rusakova, T. Ould-Ely, C. Hofmann, A. Luettge and K. H. Whitmire, *Nano Lett.*, 2007, **7**, 2920-2925.
33. A. C. Colson and K. H. Whitmire, *Organometallics*, 2010, **29**, 4611-4618.
34. D. E. Schipper, Z. Zhao, A. P. Leitner, S. L. Donaldson, A. Kumar, F. Qin, Z. Wang, J. Bao, H. Thirumalai, L. C. Grabow and K. Whitmire, H., *Chem. Mater.*, 2018, DOI: 10.1021/acs.chemmater.8b01624, in press.
35. E. Muthuswamy, P. R. Kharel, G. Lawes and S. L. Brock, *ACS Nano*, 2009, **3**, 2383-2393.
36. K. Chen, X. Huang, C. Wan and H. Liu, *RSC Adv.*, 2015, **5**, 92893-92898.
37. J. Park, B. Koo, K. Y. Yoon, Y. Hwang, M. Kang, J.-G. Park and T. Hyeon, *J. Am. Chem. Soc.*, 2005, **127**, 8433-8440.
38. S. C. Perera, G. Tsoi, L. E. Wenger and S. L. Brock, *J. Am. Chem. Soc.*, 2003, **125**, 13960-13961.
39. D. Li, H. Baydoun, C. N. Verani and S. L. Brock, *J. Am. Chem. Soc.*, 2016, **138**, 4006-4009.
40. C. Qian, F. Kim, L. Ma, F. Tsui, P. Yang and J. Liu, *J. Am. Chem. Soc.*, 2004, **126**, 1195-1198.
41. S. C. Perera and S. L. Brock, *Mater. Res. Soc. Symp. Proc.*, 2002, **755**, 129-134.
42. S. C. Perera, P. S. Fodor, G. M. Tsoi, L. E. Wenger and S. L. Brock, *Chem. Mater.*, 2003, **15**, 4034-4038.
43. K. Y. Yoon, Y. Jang, J. Park, Y. Hwang, B. Koo, J.-G. Park and T. Hyeon, *J. Solid State Chem.*, 2008, **181**, 1609-1613.
44. D.-H. Ha, L. M. Moreau, C. R. Bealing, H. Zhang, R. G. Hennig and R. D. Robinson, *J. Mater. Chem.*, 2011, **21**, 11498-11510.
45. H. Zhang, D.-H. Ha, R. Hovden, L. F. Kourkoutis and R. D. Robinson, *Nano Lett.*, 2011, **11**, 188-197.
46. L. M. Moreau, D.-H. Ha, H. Zhang, R. Hovden, D. A. Muller and R. D. Robinson, *Chem. Mater.*, 2013, **25**, 2394-2403.
47. E. Muthuswamy, G. H. L. Savithra and S. L. Brock, *ACS Nano*, 2011, **5**, 2402-2411.
48. C. M. Lukehart, S. B. Milne and S. R. Stock, *Chem. Mater.*, 1998, **10**, 903-908.
49. A. T. Kelly, C. S. Filgueira, D. E. Schipper, N. J. Halas and K. H. Whitmire, *RSC Adv.*, 2017, **7**, 25848-25854.
50. A. C. Colson and K. H. Whitmire, *Chem. Mater.*, 2011, **23**, 3731-3739.
51. K. Yasufuku and H. Yamazaki, *J. Organometal. Chem.*, 1971, **28**, 415-421.
52. H. Vahrenkamp, *Z. Naturforsch., B: Anorg. Chem., Org. Chem.*, 1975, **30B**, 814-815.

53. C. Hunger, W.-S. Ojo, S. Bauer, S. Xu, M. Zabel, B. Chaudret, L.-M. Lacroix, M. Scheer, C. Nayral and F. Delpech, *Chem. Commun.* , 2013, **49**, 11788-11790.
54. S. Bauer, C. Hunger, M. Bodensteiner, W.-S. Ojo, A. Cros-Gagneux, B. Chaudret, C. Nayral, F. Delpech and M. Scheer, *Inorg. Chem.*, 2014, **53**, 11438-11446.
55. M. Basato, E. Brescacin, E. Tondello and G. Valle, *Inorganica Chimica Acta*, 2001, **323**, 147-151.
56. P. Buchwalter, J. Rose, B. Lebeau, P. Rabu, P. Braunstein and J.-L. Paillaud, *Inorg. Chim. Acta*, 2014, **409**, 330-341.
57. P. Buchwalter, J. Rose, B. Lebeau, O. Ersen, M. Girleanu, P. Rabu, P. Braunstein and J.-L. Paillaud, *J. Nanopart. Res.*, 2013, **15**, 2132/2131-2132/2121.
58. B. J. Aylett and H. M. Colquhoun, *J. Chem. Soc., Dalton Trans.*, 1977, DOI: 10.1039/DT9770002058, 2058-2061.
59. M. M. Amini, T. P. Fehlner, G. J. Long and M. Politowski, *Chem. Mater.*, 1990, **2**, 432-438.
60. T. P. Fehlner, M. M. Amini, W. F. Stickle, O. A. Pringle, G. J. Long and F. P. Fehlner, *Chem. Mater.*, 1990, **2**, 263-268.
61. I. M. Watson, J. A. Connor and R. Whyman, *Thin Solid Films*, 1991, **196**, L21-L24.
62. D. E. Schipper, Z. Zhao, H. Thirumalai, A. P. Leitner, S. L. Donaldson, A. Kumar, F. Qin, Z. Wang, L. C. Grabow, J. Bao and K. H. Whitmire, *Chem. Mater.*, 2018, **30**, 3588-3598.
63. A. C. Colson, C.-W. Chen, E. Morosan and K. H. Whitmire, *Advanced Functional Materials*, 2012, **22**, 1850-1855.
64. P. Leitner Andrew, E. Schipper Desmond, J.-H. Chen, C. Colson Adam, I. Rusakova, K. Rai Binod, E. Morosan and H. Whitmire Kenton, *Chem. - Eur. J.*, 2017, **23**, 5565-5572.
65. D. E. Schipper, Z. Zhao, A. P. Leitner, L. Xie, F. Qin, M. K. Alam, S. Chen, D. Wang, Z. Ren, Z. Wang, J. Bao and K. H. Whitmire, *ACS Nano*, 2017, **11**, 4051-4059.
66. Z. Zhao, D. E. Schipper, A. P. Leitner, H. Thirumalai, J.-H. Chen, L. Xie, F. Qin, M. K. Alam, L. C. Grabow, S. Chen, D. Wang, Z. Ren, Z. Wang, K. H. Whitmire and J. Bao, *Nano Energy*, 2017, **39**, 444-453.
67. S. G. Shyu, J.-S. Wu, C.-C. Wu, S.-H. Chuang and K.-M. Chi, *Inorg. Chim. Acta*, 2002, **334**, 276-282.
68. T. H. W. Sun, H.-F. Wang and K.-M. Chi, *J. Mater. Chem.*, 2000, **10**, 1231-1233.
69. A. P. Leitner, J.-H. Chen, D. E. Schipper and K. H. Whitmire, *Chem. Mater.*, 2016, **28**, 7066-7071.
70. Y. Xu, R. Wu, J. Zhang, Y. Shi and B. Zhang, *Chem. Commun.*, 2013, **49**, 6656-6658.
71. P. Liu and J. A. Rodriguez, *J. Am. Chem. Soc.*, 2005, **127**, 14871-14878.
72. X. Yang, A.-Y. Lu, Y. Zhu, S. Min, M. N. Hedhili, Y. Han, K.-W. Huang and L.-J. Li, *Nanoscale*, 2015, **7**, 10974-10981.
73. Z. Zhang, B. Lu, J. Hao, W. Yang and J. Tang, *Chem. Commun.*, 2014, **50**, 11554-11557.
74. P. Jiang, Q. Liu, Y. Liang, J. Tian, M. Asiri Abdullah and X. Sun, *Angew. Chem. Int. Ed. Eng.*, 2014, **53**, 12855-12859.
75. L.-A. Stern, L. Feng, F. Song and X. Hu, *Energy Environ. Sci.*, 2015, **8**, 2347-2351.

76. Y.-P. Zhu, Y.-P. Liu, T.-Z. Ren and Z.-Y. Yuan, *Advanced Functional Materials*, 2015, **25**, 7337-7347.
77. C. Tang, R. Zhang, W. Lu, L. He, X. Jiang, M. Asiri Abdullah and X. Sun, *Adv. Mater.*, 2016, **29**, 1602441.
78. X. Yu, S. Zhang, C. Li, C. Zhu, Y. Chen, P. Gao, L. Qi and X. Zhang, *Nanoscale*, 2016, **8**, 10902-10907.
79. X.-D. Wang, Y.-F. Xu, H.-S. Rao, W.-J. Xu, H.-Y. Chen, W.-X. Zhang, D.-B. Kuang and C.-Y. Su, *Energy Environ. Sci.*, 2016, **9**, 1468-1475.
80. Y. Tan, H. Wang, P. Liu, Y. Shen, C. Cheng, A. Hirata, T. Fujita, Z. Tang and M. Chen, *Energy Environ. Sci.*, 2016, **9**, 2257-2261.
81. J. Yu, Q. Li, Y. Li, C.-Y. Xu, L. Zhen, P. Dravid Vinayak and J. Wu, *Advanced Functional Materials*, 2016, **26**, 7644-7651.
82. C. Wang, J. Jiang, T. Ding, G. Chen, W. Xu and Q. Yang, *Adv. Mater. Interfaces*, 2015, **3**, 1500454.
83. J. Kibsgaard, C. Tsai, K. Chan, J. D. Benck, J. K. Norskov, F. Abild-Pedersen and T. F. Jaramillo, *Energy Environ. Sci.*, 2015, **8**, 3022-3029.
84. P. Xiao, W. Chen and X. Wang, *Adv. Energy Mater.*, 2015, **5**, 1500985.
85. J. F. Callejas, C. G. Read, C. W. Roske, N. S. Lewis and R. E. Schaak, *Chem. Mater.*, 2016, **28**, 6017-6044.
86. Y. Shi and B. Zhang, *Chem. Soc. Rev.*, 2016, **45**, 1529-1541.
87. A. Dutta and N. Pradhan, *J. Phys. Chem. Lett.*, 2017, **8**, 144-152.
88. N. Suzuki, T. Horie, G. Kitahara, M. Murase, K. Shinozaki and Y. Morimoto, *Electrocatalysis*, 2016, **7**, 115-120.
89. C. Y. Son, I. H. Kwak, Y. R. Lim and J. Park, *Chem. Commun.*, 2016, **52**, 2819-2822.
90. Y. Yan, B. Zhao, S. C. Yi and X. Wang, *J. Mater. Chem. A*, 2016, **4**, 13005-13010.
91. D. Li, H. Baydoun, B. Kulikowski and S. L. Brock, *Chem. Mater.*, 2017, **29**, 3048-3054.
92. C. G. Read, J. F. Callejas, C. F. Holder and R. E. Schaak, *ACS Appl. Mater. Interfaces*, 2016, **8**, 12798-12803.
93. J. F. Callejas, C. G. Read, E. J. Popczun, J. M. McEnaney and R. E. Schaak, *Chem. Mater.*, 2015, **27**, 3769-3774.
94. A. Dutta, A. K. Samantara, S. K. Dutta, B. K. Jena and N. Pradhan, *ACS Energy Letters*, 2016, **1**, 169-174.
95. P. Wang, F. Song, R. Amal, H. Ng Yun and X. Hu, *ChemSusChem*, 2016, **9**, 472-477.
96. J. Wang, W. Yang and J. Liu, *J. Mater. Chem. A*, 2016, **4**, 4686-4690.
97. M. Ledendecker, S. Krick Calderón, C. Papp, H.-P. Steinrück, M. Antonietti and M. Shalom, *Angew. Chem. Int. Ed. Eng.*, 2015, **54**, 12361-12365.
98. B. You, N. Jiang, M. Sheng, M. W. Bhushan and Y. Sun, *ACS Catalysis*, 2016, **6**, 714-721.
99. A. B. Laursen, R. B. Wexler, M. J. Whitaker, E. J. Izett, K. U. D. Calvinho, S. Hwang, R. Rucker, H. Wang, J. Li, E. Garfunkel, M. Greenblatt, A. M. Rappe and G. C. Dismukes, *ACS Catalysis*, 2018, **8**, 4408-4419.
100. S. Wei, K. Qi, Z. Jin, J. Cao, W. Zheng, H. Chen and X. Cui, *ACS Omega*, 2016, **1**, 1367-1373.

101. H. von Kaenel, L. Gantert, R. Hauger and P. Wachter, *Int. J. Hydrog. Energy*, 1985, **10**, 821-827.
102. W. Zhu, C. Tang, D. Liu, J. Wang, A. M. Asiri and X. Sun, *J. Mater. Chem. A*, 2016, **4**, 7169-7173.
103. X. Chen, D. Wang, Z. Wang, P. Zhou, Z. Wu and F. Jiang, *Chem. Commun.*, 2014, **50**, 11683-11685.
104. P. Xiao, M. A. Sk, L. Thia, X. Ge, R. J. Lim, J.-Y. Wang, K. H. Lim and X. Wang, *Energy Environ. Sci.*, 2014, **7**, 2624-2629.
105. T. Liu, S. Wang, Q. Zhang, L. Chen, W. Hu and C. M. Li, *Chem. Commun.*, 2018, **54**, 3343-3346.
106. H. Duan, D. Li, Y. Tang, Y. He, S. Ji, R. Wang, H. Lv, P. P. Lopes, A. P. Paulikas, H. Li, S. X. Mao, C. Wang, N. M. Markovic, J. Li, V. R. Stamenkovic and Y. Li, *J. Am. Chem. Soc.*, 2017, **139**, 5494-5502.
107. Z. Pu, Q. Liu, A. M. Asiri and X. Sun, *ACS Appl. Mater. Interfaces*, 2014, **6**, 21874-21879.
108. M. Pi, T. Wu, D. Zhang, S. Chen and S. Wang, *Nanoscale*, 2016, **8**, 19779-19786.
109. X. Xiao, L. Tao, M. Li, X. Lv, D. Huang, X. Jiang, H. Pan, M. Wang and Y. Shen, *Chem. Sci.*, 2018, **9**, 1970-1975.
110. X. Zhang, W. Gu and E. Wang, *Nano Res.*, 2017, **10**, 1001-1009.
111. Y. Tan, H. Wang, P. Liu, Y. Shen, C. Cheng, A. Hirata, T. Fujita, Z. Tang and M. Chen, *Energy Environ. Sci.*, 2016, **9**, 2257-2261.
112. X. Wang, H. Zhou, D. Zhang, M. Pi, J. Feng and S. Chen, *J. Power Sources*, 2018, **387**, 1-8.
113. M. Qian, S. Cui, D. Jiang, L. Zhang and P. Du, *Adv. Mater.*, 2017, **29**, 1704075.
114. J. Yu, G. Cheng and W. Luo, *J. Mater. Chem. A*, 2017, **5**, 11229-11235.
115. Y. Li, H. Zhang, M. Jiang, Q. Zhang, P. He and X. Sun, *Advanced Functional Materials*, 2017, **27**, 1702513.
116. J. Kibsgaard, C. Tsai, K. Chan, J. D. Benck, J. K. Nørskov, F. Abild-Pedersen and T. F. Jaramillo, *Energy Environ. Sci.*, 2015, **8**, 3022-3029.
117. C. Jiao, M. Hassan, X. Bo and M. Zhou, *J. Alloys Cmpds.*, 2018, **764**, 88-95.
118. J. Lin, C. Wang, S. Wang, Y. Chen, W. He, T. Ze and B. Chen, *J. Alloys Cmpds.*, 2017, **719**, 376-382.
119. M. Pi, D. Zhang, S. Wang and S. Chen, *Mater. Lett.*, 2018, **213**, 315-318.
120. C. Guan, W. Xiao, H. Wu, X. Liu, W. Zang, H. Zhang, J. Ding, Y. P. Feng, S. J. Pennycook and J. Wang, *Nano Energy*, 2018, **48**, 73-80.
121. K. Tang, X. Wang, M. Wang, Y. Xie, J. Zhou and C. Yan, *ChemElectroChem*, 2017, **4**, 2150-2157.
122. L. Wei, K. Goh, Ö. Birer, H. E. Karahan, J. Chang, S. Zhai, X. Chen and Y. Chen, *Nanoscale*, 2017, **9**, 4401-4408.
123. Y. Yang, K. Zhou, L. Ma, Y. Liang, X. Yang, Z. Cui, S. Zhu and Z. Li, *Appl. Surf. Sci.*, 2018, **434**, 871-878.
124. X.-D. Wang, H.-Y. Chen, Y.-F. Xu, J.-F. Liao, B.-X. Chen, H.-S. Rao, D.-B. Kuang and C.-Y. Su, *J. Mater. Chem. A*, 2017, **5**, 7191-7199.
125. D. R. Liyanage, D. Li, Q. B. Cheek, H. Baydoun and S. L. Brock, *J. Mater. Chem. A*, 2017, **5**, 17609-17618.